

HETEROCYCLES, Vol. 74, 2007, pp. 607 - 616. © The Japan Institute of Heterocyclic Chemistry
Received, 21st August, 2007, Accepted, 23rd October, 2007, Published online, 26th October, 2007. COM-07-S(W)38

SYNTHESIS, CRYSTAL STRUCTURE, AND MAGNETIC PROPERTIES OF 4-(2-METHYL-1-AZASPIRO[4.5]DECA-1-OXYL-2-YL)PHENOL

Yoshiaki Uchida, Nagahisa Matsuoka, Hiroki Takahashi, Satoshi Shiono,
Naohiko Ikuma, and Rui Tamura*

Graduate School of Human and Environmental Studies, Kyoto University, Kyoto
606-8501, Japan

Corresponding author; e-mail: tamura-r@mbox.kudpc.kyoto-u.ac.jp

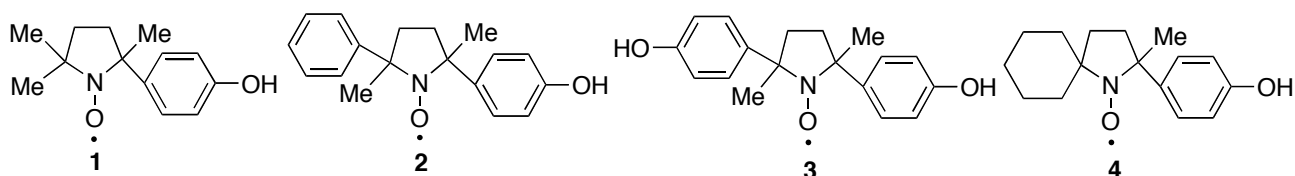
Abstract – The two polymorphic forms (α and β) of the racemate of the title chiral nitroxide radical were separately obtained by changing the composition ratio of the recrystallization solvent (hexane/Et₂O). Both polymorphs existed as a racemic compound; the thermally less stable α -form was monoclinic (space group, *C2/c*), and the stable β -form was orthorhombic (*Pbca*). The origin of the formation of the racemic compound crystals for the α - and β -forms was interpreted in terms of the formation of a strong intermolecular head-to-tail type of hydrogen bond between a nitroxyl group and the nearest hydroxy group in a pair of *R* and *S* enantiomers giving a heterochiral cyclic dimer and a heterochiral 1D chain, respectively, by X-ray crystallographic analysis. Furthermore, magnetic susceptibility measurements of the two polymorphs indicated the presence of weak antiferromagnetic interactions, which were rationalized in terms of the formation of homochiral and heterochiral 1D chains in the crystal structures of the α - and β -forms, respectively, by DFT calculations.

INTRODUCTION

With a view to utilizing a chiral five-membered cyclic nitroxide framework as a spin source for (i) the elaboration of chiral paramagnetic liquid crystals¹⁻³ and (ii) the building of chiral multispin system on the cyclotriphosphazene scaffold,^{4,5} as well as to providing a new chiral spin-labeling reagent for EPR spectroscopic studies, we synthesized racemic and enantiomerically enriched nitroxides **1**, *trans*-**2**, and *trans*-**3** with one or two 4-hydroxyphenyl groups on the stereogenic centers.⁶⁻⁸ Interestingly, racemic **1**, *trans*-**2**, and *trans*-**3** were found to exist as a racemic conglomerate (an equal mixture of *R* and *S* chiral crystals), which is very rare for chiral nitroxide radicals.^{6,7} The origin of the conglomerate formation with

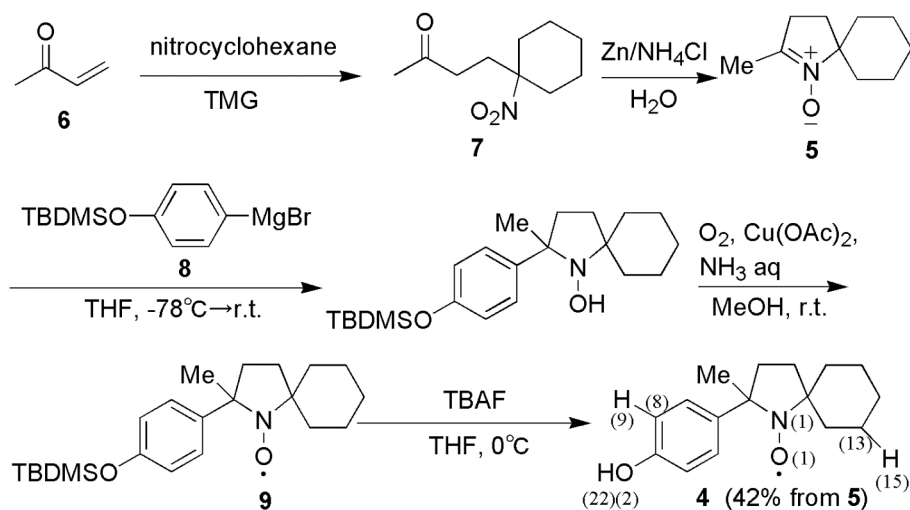
respect to these racemates was interpreted in terms of the existence of homochiral 1D chains formed by the strong intermolecular hydrogen bonds between the hydroxy (OH) and nitroxyl (NO) groups, together with weak attractive forces such as dipole-dipole interactions between two NO groups and C(spⁿ)H...ON interactions.^{6,7}

Here we report that the two polymorphic (α and β) forms of novel racemic 4-(2-methyl-1-azaspiro[4.5]deca-1-oxyl-2-yl)phenol (**4**), a spiro analogue of **1**, exist as a racemic compound, despite the existence of a 4-hydroxyphenyl group attached to the stereogenic center of the pyrrolidine ring. The origin of the formation of the racemic compound crystals has been studied by X-ray crystallographic analysis, magnetic susceptibility measurements, and DFT calculations.



RESULTS AND DISCUSSION

Synthesis. Racemic **4** was synthesized from known racemic 2-methyl-1-azaspiro[4.5]deca-1-ene 1-oxide (**5**)⁹⁻¹² by a procedure similar to the synthesis of **1** (Scheme 1).^{6,7} Reaction of **5** with the Grignard reagent **8** and the subsequent oxidation gave (\pm)-**9**, which was further desilylated with tetrabutylammonium fluoride (TBAF) to afford (\pm)-**4**.



Scheme 1. Synthesis of (\pm)-**4**

Control of polymorphism. Rapid evaporation of a solution of (\pm)-**4** in hexane/Et₂O (v/v = 10/1) in vacuo afforded a mixture of clumped and needle-like crystals. The differential scanning calorimetry (DSC) analysis of the polymorphic mixture exhibited two endothermic peaks on the heating run (Figure 1). The clumped and needle-like crystals were named α - and β -forms, respectively.

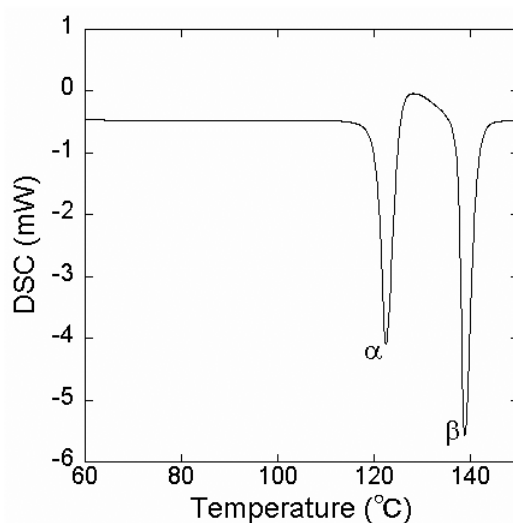


Figure 1. DSC curve of the polymorphic mixture of (±)-**4** on the heating run.

The two polymorphic forms were separately obtained by changing the composition ratio of the recrystallization solvent (hexane/Et₂O). The α -form was prepared by recrystallization from a 15:4 mixture of hexane and Et₂O (10 mg/mL), while the β -form was produced by recrystallization from a 3:15 mixture of hexane and Et₂O (10 mg/mL). The α - and β -forms showed sharp endothermic peaks at 122 °C and 138 °C by DSC analysis, respectively (Figure 2). Thus, the α - and β -forms turned out to be thermally less stable and more stable forms, respectively.

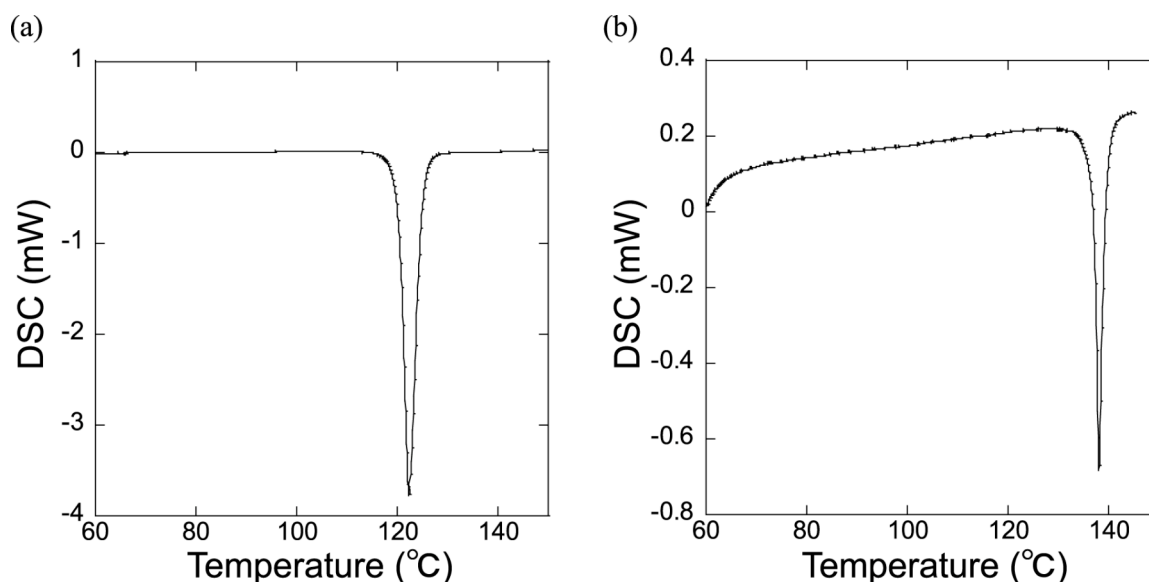


Figure 2. DSC curves of (a) the α -form and (b) the β -form of (±)-**4**.

Crystal structures. The crystal structures of both α and β forms of (±)-**4** were determined by X-ray crystallographic analysis. The α - and β -forms crystallized as a racemic compound in respective space groups of *C2/c* and *Pbca*, which have a single molecule in the asymmetric unit. The crystal structure of the α -form was characterized by (i) the heterochiral dimers formed through the strong hydrogen bond

between a nitroxyl group and the nearest OH group (O(1)---O(2) distance: 2.760 Å) and the π/π interactions (centroid---centroid distance: 3.741 Å) between the nearest two benzene rings on the *ac* plane (Figure 3a) as well as (ii) the homochiral 1D chain along the *b* axis formed by the weak C(sp³)H---O contact between a nitroxyl group and the nearest cyclohexyl ring (O(1)---C(13) distance: 3.450 Å) (Figure 3b). On the other hand, the crystal structure of the β -form consisted of the heterochiral 1D chain along the *c* axis formed through (i) the hydrogen bond between a nitroxyl group and the nearest OH group (O(1)---O(2) distance: 2.720 Å) and (ii) the weak C(sp²)H---O contact between a nitroxyl group and the nearest phenol ring (O(1)---C(8) distance: 3.307 Å) (Figure 4).

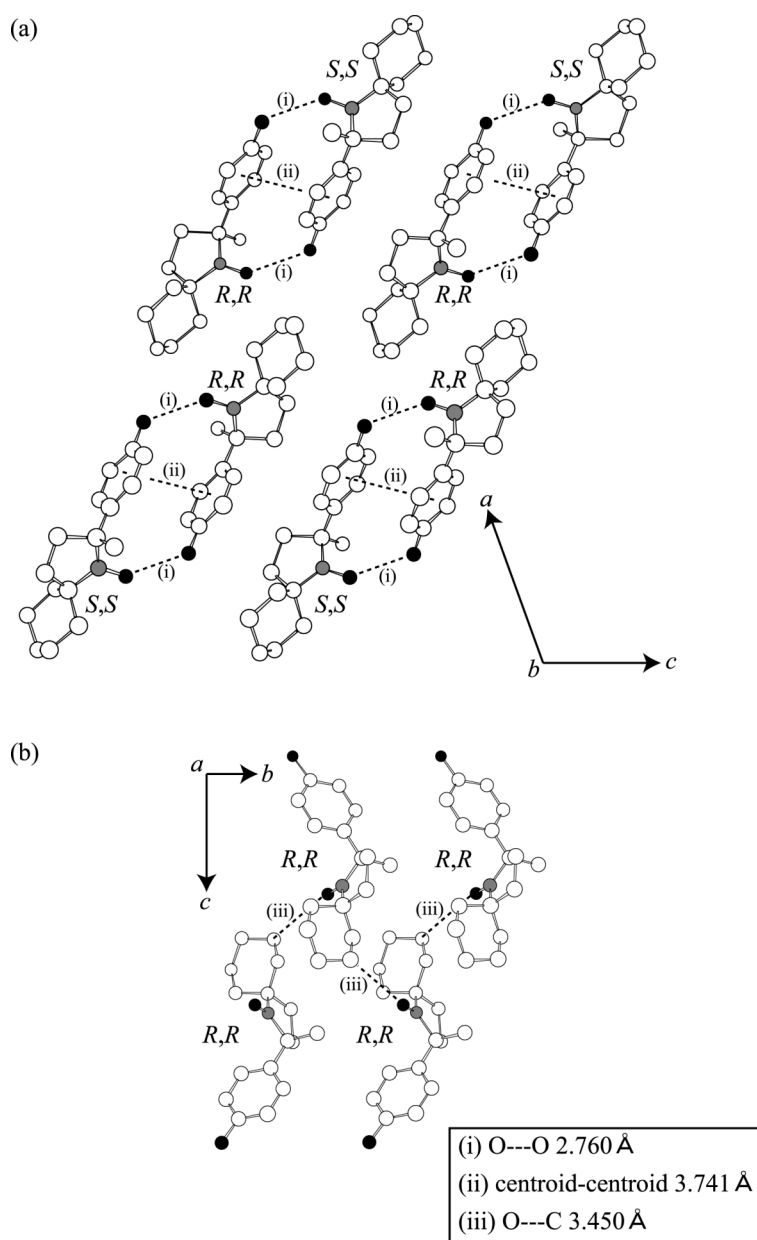


Figure 3. Crystal structure of the α -form of (\pm)-**4** viewed down a) the *b* axis and b) the *a* axis. (i) N(1)–O(1)---H(22)–O(2) interactions. (ii) π/π interactions. (iii) N(1)–O(1)---H(15)–C(13) interactions. Carbon, nitrogen, and oxygen atoms are denoted by white, gray, and black circles, respectively.

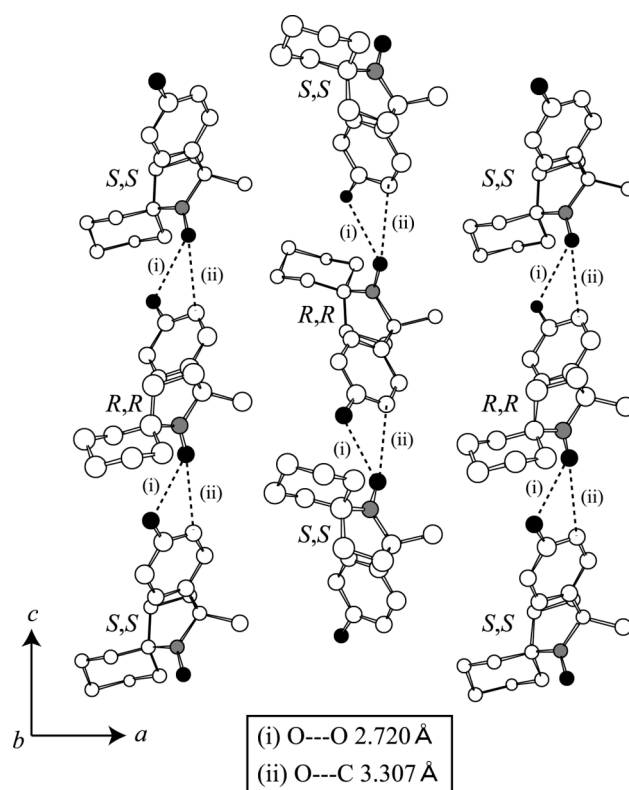


Figure 4. Crystal structure of the β -form of (\pm)-**4** viewed down the b axis. (i) N(1)–O(1)---H(22)–O(2) interactions. (ii) N(1)–O(1)---H(9)–C(8) interactions. Carbon, nitrogen, and oxygen atoms are denoted by white, gray, and black circles, respectively.

Table 1. Crystallographic data of two polymorphic forms of (\pm)-**4**.

	α -form	β -form
Empirical Formula	C ₁₆ H ₂₂ O ₂ N	C ₁₆ H ₂₂ O ₂ N
Formula Weight	260.36	260.36
Crystal Color, Habit	yellow, block	brown, prism
Crystal Dimensions	0.60 x 0.60 x 0.60 mm	0.50 x 0.30 x 0.30 mm
Crystal System	Monoclinic	Orthorhombic
Lattice Parameters	$a = 25.382(4) \text{ \AA}$ $b = 6.5431(7) \text{ \AA}$ $c = 17.724(2) \text{ \AA}$ $\beta = 109.928(9)^\circ$ $V = 2767.4(6) \text{ \AA}^3$	$a = 13.899(7) \text{ \AA}$ $b = 12.957(6) \text{ \AA}$ $c = 15.928(9) \text{ \AA}$ $V = 2868(2) \text{ \AA}^3$
Space Group	$C2/c$ (#15)	$Pbca$ (#61)
Z value	8	8
R value	0.046	0.036
Rw value	0.050	0.036

Magnetic properties. The temperature dependence of magnetic susceptibility of the α - and β -form crystals of (\pm)-**4** was measured between 2.0 and 300 K with an applied magnetic field of 5000 Oe on a SQUID magnetometer (Figure 5), because this measurement often affords useful information on weak intermolecular interactions in the crystal lattice.^{13,14} Their magnetic behaviors were best fitted to a 1D regular Heisenberg model of $S = 1/2$,¹⁵ which is described by

$$\chi = \frac{Ng^2\mu_B^2}{kT} \frac{0.25 + 0.074975x + 0.075235x^2}{1 + 0.9931x + 0.172135x^2 + 0.757825x^3} \quad (\text{Eq. 1})$$

with

$$x = |J|/kT \quad (\text{Eq. 2})$$

where N stands for Avogadro constant, g for g -value, μ_B for Bohr magneton, and k for Boltzmann constant. The α - and β -forms of (\pm)-**4** showed antiferromagnetic interactions with $J/k = -3.54 \pm 0.05$ K and $J/k = -3.04 \pm 0.02$ K, respectively. Therefore, the existence of the respective homochiral or heterochiral 1D chain for the α - or β -form of (\pm)-**4** is most likely responsible for such distinct intermolecular antiferromagnetic interactions observed (Figure 3b and Figure 4).

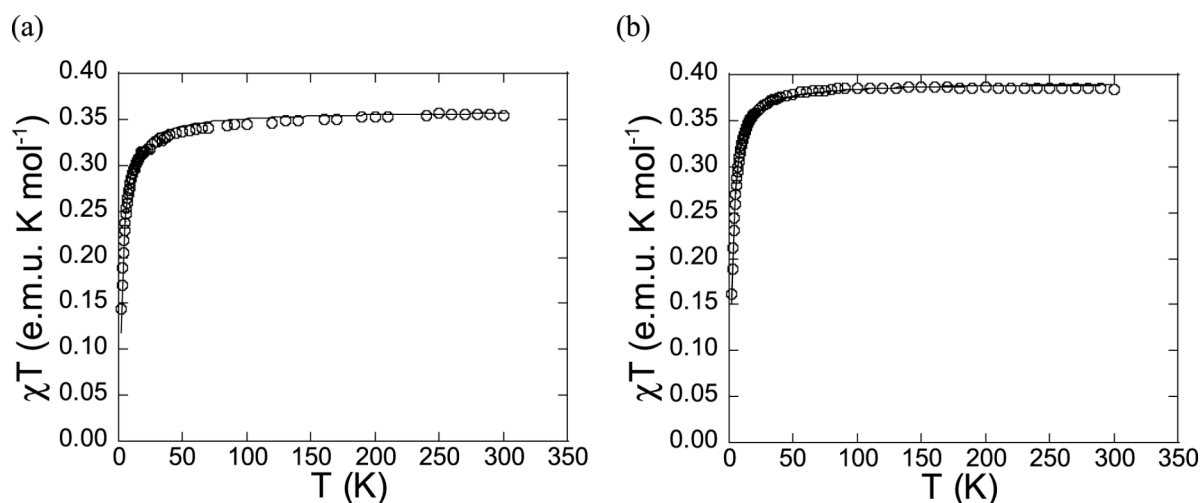


Figure 5. Temperature dependence of χT for (a) α -form and (b) β -form of (\pm)-**4**. The solid lines indicate theoretical curves.

To confirm this assumption, we performed a DFT calculation to reveal the spin density distributions using PC SPARTAN '02. For the computation, the popular unrestricted B3LYP hybrid function with the 6-31G** basis set was used on the coordinates obtained by the X-ray analysis. Figure 6 shows the calculated spin density distributions for the α - and β -form molecules of **4**. The calculated spin densities are summarized in Table 2. The nitrogen and oxygen atoms of the nitroxyl groups have overwhelmingly larger spin densities than the other atoms. Therefore, an orbital overlap between the nitroxyl group and one or more atoms with a larger spin density in the neighboring molecule should result in intermolecular antiferromagnetic interactions.¹⁶ In the case of the α -form molecule, the nitroxyl group N(1)–O(1) has

close contacts with H(22)–O(2) and H(15)–C(13) in the neighboring molecules. The latter H(15)–C(13) has larger spin densities than the former H(22)–O(2). Therefore, the hydrogen bond between N(1)–O(1) and H(15)–C(13) resulting in the homochiral 1D chain along the *b* axis (Figure 3b) is responsible for the antiferromagnetic interactions. Similarly, in the case of the β -form molecule, the nitroxyl group N(1)–O(1) has close contacts with H(22)–O(2) and H(9)–C(8) in a neighboring molecule. The latter H(9)–C(8) has larger spin densities than the former H(22)–O(2). Therefore, the antiferromagnetic interactions arise from the hydrogen bond between N(1)–O(1) and H(9)–C(8) forming a heterochiral 1D chain along the *c* axis (Figure 4). These results are consistent with the magnetic behavior described.

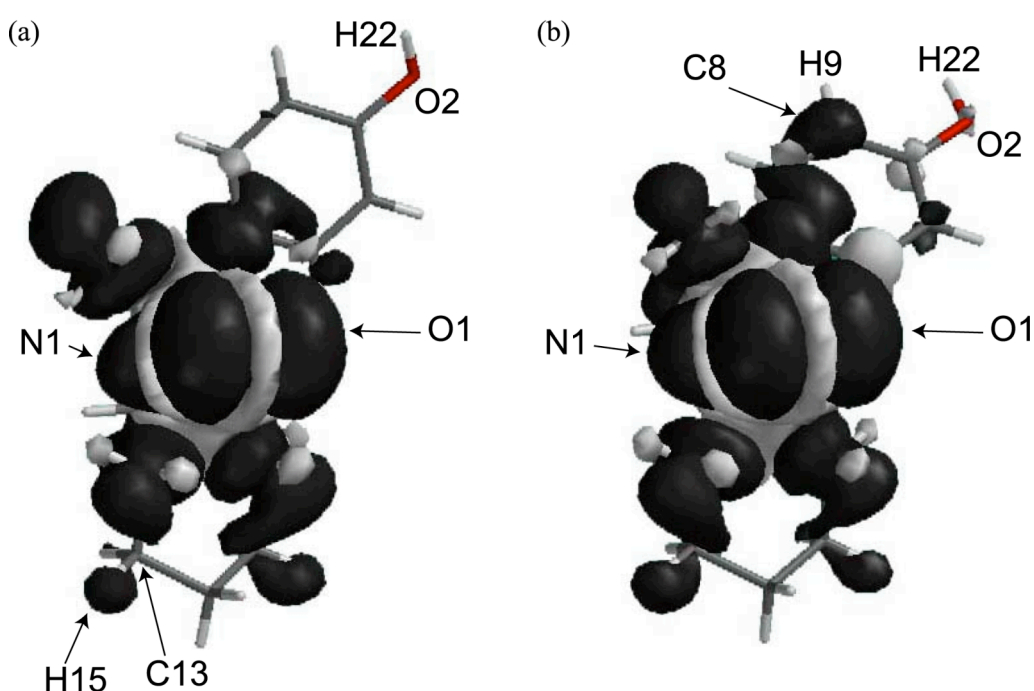


Figure 6. Spin density distributions of (a) α -form and (b) β -form molecules of **4**. Computations were performed at the unrestricted B3LYP/6-31G** level. Positive and negative spin densities are denoted by black and white, respectively.

Table 2. Calculated spin density distributions of α - and β -form molecules of **4**.

α -form		β -form	
Site	Density	Site	Density
N(1)	0.445418	N(1)	0.449633
O(1)	0.521982	O(1)	0.520295
C(13)	-0.000156	C(8)	0.002428
H(15)	0.000901	H(9)	0.000132
H(22)	0.000004	H(22)	-0.000001
O(2)	-0.000122	O(2)	-0.000226

In summary, we separately obtained the two polymorphic forms of the racemic nitroxide radical **4**. The strong intermolecular OH---ON hydrogen bonds together with weak attractive forces such as C(spⁿ)H---ON turned out to be responsible for the formation of the racemic compound crystals. Furthermore, the intermolecular antiferromagnetic interactions observed for both polymorphs were rationalized in terms of the formation of a homochiral or heterochiral 1D chain by means of X-ray crystallographic analysis and DFT calculations.

EXPERIMENTAL

General. Unless otherwise noted, solvents and reagents were reagent grade and used without purification (or after dried by molecular sieves 4A). THF for electron paramagnetic resonance (EPR) spectroscopy or Grignard reactions was distilled from sodium/benzophenone ketyl under argon. 3-Buten-2-one for the synthesis of 4-(1-nitrocyclohexyl)butan-2-one was distilled. DSC was performed at a scanning rate of 5°C/min using SHIMADZU DSC-50. Melting points were determined by micro melting point apparatus (Yanako MP-500D). IR spectra were recorded with SHIMADZU FT-IR8600PC and SHIMADZU IRPrestige-21. EPR spectra were recorded with a JEOL FE1XG. Magnetizations were recorded with QUANTUN DESIGN MPMS-2 and MPMS-5S. DFT calculations at UB3LYP/6-31G** level were performed by SPARTAN '02 for Windows. SHIMADZU LC-10ATVP, SPD-10AVP, and C-R8A were used for HPLC analyses.

Synthesis. To a stirred solution of 3-buten-2-one (**6**) (0.300 g, 4.0 mmol) and nitrocyclohexane (1.55 g, 12 mmol) at 0°C was added dropwise 1,1,3,3-tetramethylguanidine (TMG) (0.138 g, 1.2 mmol). The temperature was raised slowly to rt, and stirring was continued overnight. It was then diluted with Et₂O and washed successively with aqueous hydrochloric acid (2 N), saturated aqueous NaHCO₃, and saturated brine, and then dried over MgSO₄ and concentrated in vacuo to give crude 4-(1-nitrocyclohexyl)butan-2-one (**7**) (0.786 g, 3.9 mmol, 99 %) as a colorless oil. Compound **7** is known.¹²

To a stirred suspension of **7** (0.786 g, 3.9 mmol) and NH₄Cl (0.171 g, 3.2 mmol) in water (4 mL) was added zinc powder (0.836 g, 13 mmol) in small portions over a period of 30 min at such a rate that the reaction temperature did not exceed 10 °C. The reaction mixture was stirred at 0 °C for an additional 3.5 h, and filtered. The filtrate was combined with several methanol washes of the filter cake. The filtrate was concentrated under reduced pressure, and then extracted with CH₂Cl₂. The combined organic phase was dried over MgSO₄ and concentrated in vacuo. The residual oil was carefully dried by azeotropic removal of water by the evaporation of the remaining trace of benzene under 3 mmHg to afford the known compound **5** (0.501 g, 3.0 mmol, 77 %) as a colorless oil.¹²

Compound **5** (0.501 g, 3.0 mmol) was dissolved in THF under argon and cooled down to $-78\text{ }^{\circ}\text{C}$. Two equiv of Grignard reagent **8** was dropwise added to the solution. The reaction mixture was slowly warmed to $25\text{ }^{\circ}\text{C}$, stirred overnight, and poured into saturated aqueous NH_4Cl . The aqueous phase was extracted with CH_2Cl_2 . The combined organic phase was dried over MgSO_4 and concentrated in vacuo. To the residue dissolved in MeOH (12 mL) was added conc. aqueous NH_3 (1 mL) and $\text{Cu}(\text{OAc})_2\cdot\text{H}_2\text{O}$ (0.120 g, 0.60 mmol). Oxygen was bubbled through the solution until its color became dark blue. After the solvent was evaporated, the residue was dissolved in saturated aqueous NaHCO_3 and the aqueous phase was extracted with CH_2Cl_2 . The combined organic phase was dried over MgSO_4 and concentrated in vacuo. The crude product was purified by column chromatography (silica gel, hexane/ Et_2O 19/1) to give a crude yellow solid of (\pm)-**9**. To the crude nitroxide (\pm)-**9** dissolved in THF (15 mL) was added 2 mL of TBAF (1 M solution in THF) at $0\text{ }^{\circ}\text{C}$. After stirring 1 h, the reaction mixture poured into saturated aqueous NH_4Cl , and the aqueous phase was extracted with Et_2O . The combined organic phase was dried over MgSO_4 and concentrated in vacuo. Column chromatography (silica gel, $\text{CH}_2\text{Cl}_2/\text{Et}_2\text{O}$ 10/1) of the residue gave (\pm)-**4** as a pure yellow solid in 42% yield from **5**.

The α -form of (\pm)-**4** was obtained by recrystallization from a mixed solvent of hexane and Et_2O (v/v 15:4, 10 mg/mL), while the β -form was similarly obtained by recrystallization from a 3:15 (v/v) mixture of hexane and Et_2O (10 mg/mL). The α -form was clumped crystal, and the β -form was needle-like crystal.

(\pm)-**4**: EPR (THF): $g = 2.0064$, $a_{\text{N}} = 1.30\text{ mT}$. IR (KBr): 619, 708, 836, 1176, 1272, 1366, 1456, 1513, 1595, 1617, 2934, 3181. Anal. Calcd for $\text{C}_{16}\text{H}_{22}\text{NO}_2$: C, 73.81; H, 8.52; N, 5.38. Found: C, 73.55; H, 8.60; N, 5.35. Mp: α -form, $119.57\text{--}125.35\text{ }^{\circ}\text{C}$; β -form, $137.01\text{--}139.48\text{ }^{\circ}\text{C}$.

Crystallography. The X-ray crystallographic data were collected at 100 K in a Rigaku RAXIS RAPID imaging plate. The crystal structure was solved by direct methods and refined by full-matrix least squares. All non-hydrogen atoms were refined anisotropically. All of the crystallographic calculations were performed by using the CrystalStructure software package. The summary of the fundamental crystal data for the structure determination is given in Table 1. The experimental details including data collection, data reduction, and structure solution and refinement as well as the atomic coordinates and Biso/Beq, anisotropic displacement parameters, have been deposited in the Supporting Information. CCDC-656895 and 656896 contain the supplementary crystallographic data for this paper. These data can be obtained free of charge via www.ccdc.cam.ac.uk/conts/retrieving.html (or from the Cambridge Crystallographic Data Centre, 12 Union road, Cambridge CB21EZ, UK; fax: (+44)1223-336-033; or e-mail: deposit@ccdc.cam.ac.uk).

REFERENCES (AND NOTES)

1. N. Ikuma, R. Tamura, S. Shimono, N. Kawame, O. Tamada, N. Sakai, J. Yamauchi, and Y. Yamamoto, *Angew. Chem. Int. Ed.*, 2004, **43**, 3677.
2. N. Ikuma, R. Tamura, K. Masaki, Y. Uchida, S. Shimono, K. Masaki, J. Yamauchi, Y. Aoki, and H. Nohira, *Adv. Mater.*, 2006, **18**, 477.
3. N. Ikuma, R. Tamura, S. Shimono, Y. Uchida, J. Yamauchi, Y. Aoki, and H. Nohira, *Ferroelectrics*, 2006, **343**, 119.
4. S. Shimono, R. Tamura, N. Ikuma, H. Takahashi, N. Sakai, and J. Yamauchi, *Chem. Lett.*, 2004, **33**, 932.
5. S. Shimono, H. Takahashi, N. Sakai, R. Tamura, N. Ikuma, and J. Yamauchi, *Mol. Cryst. Liq. Cryst.*, 2005, **440**, 37.
6. N. Ikuma, R. Tamura, S. Shimono, N. Kawame, O. Tamada, N. Sakai, J. Yamauchi, and Y. Yamamoto, *Mendeleev Commun.*, 2003, 109.
7. N. Ikuma, R. Tamura, S. Shimono, N. Kawame, O. Tamada, N. Sakai, Y. Yamamoto, and J. Yamauchi, *Mol. Cryst. Liq. Cryst.*, 2005, **440**, 23.
8. N. Ikuma, H. Tsue, N. Tsue, S. Shimono, Y. Uchida, K. Masaki, N. Matsuoka, and R. Tamura, *Org. Lett.*, 2005, **7**, 1797.
9. H. Shechter, D. F. Ley, and L. Zeldin, *J. Am. Chem. Soc.*, 1952, **74**, 3664.
10. P. G. Baraldi, A. Barco, S. Benetti, G. P. Pollini, and D. Simoni, *Tetrahedron*, 1987, **43**, 4669.
11. G. R. Delpierre and M. Lamchen, *J. Chem. Soc.*, 1963, 4693.
12. E. Lint, Nitro Compound, Proceedings of the International Symposium, 1964, 291.
13. 'Magnetism: Molecules to Materials II,' eds. by J. S. Miller and M. Drillon, Wiley-VCH, Weinheim, 2001.
14. 'Magnetic Properties of Organic Molecules,' ed. by P. M. Lahti, Marcel Dekker, New York, 1999.
15. O. Kahn, 'Molecular Magnetism,' VHC Publishers, Inc., New York, 1993, pp. 252-286.
16. Y. Uchida, R. Tamura, N. Ikuma, K. Masaki, H. Takahashi, S. Shimono, and J. Yamauchi, *Mendeleev Commun.*, 2006, 69.